Laser Frequency-Offset Locking at 10-Hz-Level Instability Using Hybrid Electronic Filters

Vyacheslav Li, Fritz Diorico, and Onur Hosten*
Institute of Science and Technology Austria, Am Campus 1, Klosterneuburg 3400, Austria

(Received 26 November 2021; revised 1 March 2022; accepted 11 April 2022; published 19 May 2022)

Lasers with well-controlled relative frequencies are indispensable for many applications in science and technology. We present a frequency-offset locking method for lasers based on beat-frequency discrimination utilizing hybrid electronic *LC* filters. The method is specifically designed for decoupling the tightness of the lock from the broadness of its capture range. The presented demonstration locks two free-running diode lasers at 780 nm with a 5.5-GHz offset. It displays an offset frequency instability below 55 Hz for time scales in excess of 1000 s and a minimum of 12 Hz at 10-s averaging. The performance is complemented with a 190-MHz lock-capture range, a tuning range of up to 1 GHz, and a frequency ramp agility of 200 kHz/μs.

DOI: 10.1103/PhysRevApplied.17.054031

I. INTRODUCTION

The ability to generate laser beams with well-controlled and stable relative frequencies enables applications in many areas of science and technology. Precision optical metrology using optical-frequency combs [1], laser cooling and trapping of atoms [2], coherent manipulation of their internal [3] as well as their motional degrees of freedom [4,5], and coherent manipulation of solid-state quantum systems [6,7] are examples that rely on good relative-frequency control. The capability of controlling such systems makes possible precision applications such as atomic clocks [8] and atom interferometers [9] for geodesy, inertial navigation, and tests of fundamental physics [10] and makes possible many quantum information processing applications.

A number of general techniques exist for generating laser tones with fixed relative frequencies. These include splitting a single laser beam and shifting its frequency with acousto-optic [11] or electro-optic modulators (EOMs) [12]—reaching offsets from tens of megahertz to tens of gigahertz—locking separate lasers to different resonances of optical cavities [13] or atomic systems [14,15]—reaching from gigahertz to hundreds of terahertz—and directly stabilizing the frequency offset between lasers by utilizing the interference beat note between the optical tones on a photodetector—which offers the largest range of applicability while keeping the lasers spectrally pure. This last technique forms the basis of the method developed in the present work.

A direct beat note between two lasers can be detected at up to tens of gigahertz on fast photodiodes and offsets up to a couple of hundred gigahertz are achievable by beating one of the lasers with a high-order sideband of another laser resulting from its phase modulation with an EOM [16]. Octave-spanning offset frequencies all the way up to the terahertz range can be achieved by utilizing the beat notes of two lasers with different spectral lines of an optical-frequency comb [17], enabling optical clock-frequency comparison.

In principle, phase locking of two lasers with the aid of an optical beat note [18,19] produces the tightest frequency lock, reaching below submillihertz instability levels. However, this optical-phase-locked loop (OPLL) method places the most stringent demands on the feedback-stabilization bandwidths, requiring them to be appreciably larger than the line width of the lasers. This makes OPLLs especially challenging with semiconductor diode-laser systems, which possess line widths from several hundred kilohertz to several tens of megahertz. Nevertheless, many applications do not require phase locking, in which case the laser frequencies can more easily be steered and locked using purely beat-frequency discrimination—instead of phase discrimination.

Among typically utilized discriminators, simple delay-line based architectures [20,21] have been demonstrated to reach 1-kHz-frequency-difference instability but they suffer from technical complications due to periodically repeating locking points. Digital counting architectures [22] have been demonstrated to reach 300-Hz instability but suffer from implementation complexity and spurious digital noise (which could disturb the laser power spectral density and negatively affect short-term

*onur.hosten@ist.ac.at

stability). Architectures relying on integrated frequency-to-voltage-conversion circuits have reached instabilities in the (30–100)-Hz range but they also suffer from implementation complexities that come about, overcoming the limited frequency range (approximately 1 MHz) of such chips. Similarly, side-of-filter-type architectures [23–25] have also been demonstrated to reach down to the 100-Hz instability regime. Basic implementations of these architectures typically trade off locking stability with the initial capture range of the lock, posing a general additional limitation.

Here, we develop a frequency-discrimination method based on hybrid *LC* filters for laser offset locking. The method is developed with the following goals: obtaining a single lockable point with simultaneous wide-tunability, high locking stability, and a broad capture range. The implemented frequency discriminator (FD) generates an error signal with a 1.8-MHz-wide steep region and broad tails that extend out to hundreds of megahertz, to ensure a large capture range. The all-analog design of the offset locking circuitry ensures low-noise operation. An offset frequency tunability of 1 GHz is incorporated by heterodyning the beat signal with a tunable microwave local oscillator (LO) generated from a direct digital synthesizer (DDS).

We demonstrate the developed method on two 780-nm miniature external-cavity diode lasers (ECDLs) with observed free-running line widths of approximately 500 kHz. We stabilize the frequency offset between the two lasers at around 5.5 GHz and reach a frequency-locking instability of 12 Hz at 10 s averaging time. This value corresponds to a fractional instability of 3×10^{-14} when scaled to the laser frequency. The long-term instability remains below 55 Hz for more than 1000 s. These results constitute a very low beat-note-based offset locking instability without optical phase locking. Beyond its exceptional stability, the laser frequency offset is tunable at rates exceeding 200 kHz/μs by frequency ramping the DDS generating the LO. We note that the use of a simple *LC* circuit for laser offset locking has also been reported recently in Ref. [26] but the operation was limited to approximately 2-kHz instability levels. Below, we first detail our scheme and then describe the experimental characterization of its performance.

II. THE SCHEME

Figure 1 shows a block diagram of the laser offset frequency-locking scheme. Small portions of two lasers are superimposed on a 12-GHz-bandwidth photodetector and the resulting beat note is amplified and heterodyned with a microwave LO. The frequency down-converted signal is further amplified and its power is actively stabilized. This signal is then fed into the hybrid electronic FD to generate a baseband error signal that has opposite polarities on opposite sides of the desired frequency-offset point. A home-built feedback controller is then used to stabilize the frequency of one of the lasers at this controllable offset point with respect to the other laser. The down-conversion process that brings the beat signal from the gigahertz regime to the megahertz regime eases further electronic processing of the signal. At the same time, it enables the wide-range tunability of the frequency offset through induced changes in the LO frequency.

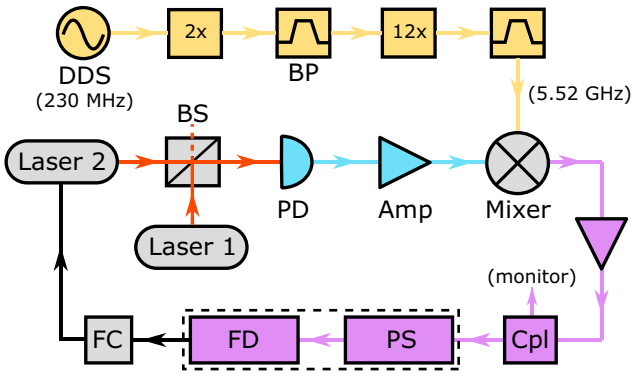

FIG. 1. A block diagram of the frequency-offset locking setup. The two lasers form a beat note on a fast photodetector (PD). The signal at approximately 5.5 GHz frequency difference (blue) is amplified and mixed down with a local oscillator (LO) chain (yellow) that starts with a direct digital synthesizer (DDS). The down-converted output (purple) of the mixer is in the megahertz range and is amplified to the saturation point. A directional coupler (Cpl) is used to monitor the beat note. The signal goes through an active power-stabilization (PS) unit to stabilize the power at the input of the frequency discriminator (FD). The feedback controller (FC) then manipulates the current of Laser 2 to stabilize its frequency at a well-defined offset from that of Laser 1: BP, band-pass filter; BS, beam splitter. Additional amplifiers in the LO chain are omitted from the diagram. Part list: PD, Thorlabs DX12CF; Amp, Mini-circuits ZX60-83LN-s+ and ZX60-43-s+; Mixer, ZX05-83-s+; Cpl, ZFDC-10-1-s+; 2×, ZX90-2-13-s+; 12×, ZX90-12-63-s+; DDS, Artiq Urukul; Lasers 1 and 2, Sacher Micron.

The FD [Fig. 2(a)] is the key component that generates the error signal with a tight resonance and a wide capture range. It is a self-mixing circuit with a specially designed hybrid filter in one of the two split arms. The input signal of the form $\sin(\omega t + \phi_0)$ is distributed into the arms with a two-way 90° power splitter. Here, ω is the angular frequency and ϕ_0 is an arbitrary phase. The arm with the hybrid filter contains the waveform $\sin(\omega t + \phi_0) \equiv \mathrm{Re}[i\, e^{-i(\omega t+\phi_0)}]$, while the other arm contains the $\cos(\omega t + \phi_0)$ waveform. The filter transforms the incoming waveform with its transfer function $H(\omega) = H_{\mathrm{Re}}(\omega) + iH_{\mathrm{Im}}(\omega)$, resulting in the transmitted signal $\mathrm{Re}[H(\omega)\, i\, e^{-i(\omega t+\phi_0)}] = H_{\mathrm{Re}}(\omega)\sin(\omega t + \phi_0) - H_{\mathrm{Im}}(\omega)\cos(\omega t + \phi_0)$. This is then combined on a frequency mixer with the $\cos(\omega t + \phi_0)$

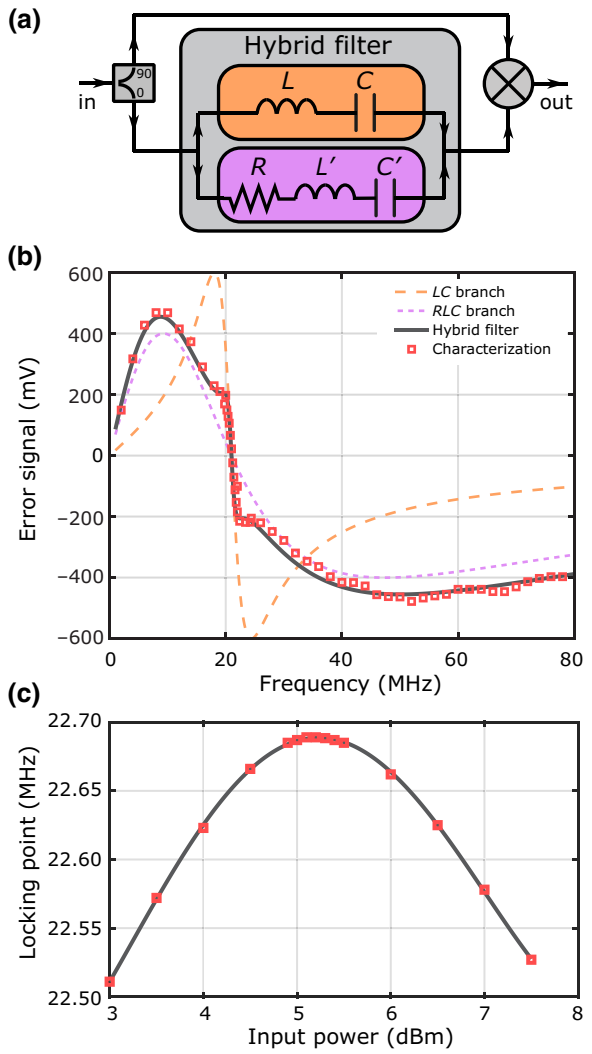

FIG. 2. (a) A schematic drawing of the FD. The hybrid filter (gray box) is composed of two branches: one *LC* filter (orange box) and one *RLC* filter (purple box). It is part of a self-mixing circuit composed of a splitter (Mini-circuits PSCQ-2-51W+1) and a mixer (RPD-1+1 phase detector). The surface-mount component values are $L = 2.2$ μH and $C = 20$ pF, and $R = 50$ Ω, $L' = 470$ nH, and $C' = 91$ pF. (b) The expected and observed frequency ($\omega/2\pi$) responses of the FD given by the imaginary part of the transfer function $H_{\mathrm{Im}}(\omega)$, corresponding to the error signal. The theoretical response curves are scaled in magnitude to fit the experimentally characterized response (red squares). Contributions of individual branches are also explicitly indicated. (c) The zero-crossing frequency of the generated error signal as a function of the input signal power at the FD (red squares) and a polynomial fit (solid line). All characterizations are carried out with a frequency-stepped tone from a function generator.

waveform coming from the other arm, to result in the baseband signal proportional to $H_{\mathrm{Im}}(\omega)$ at the mixer output, which is used as the error signal [Fig. 2(b)].

The hybrid *LC* filter design eliminates the usual trade-off between lock tightness and capture range. The *LC* circuit contained in the upper branch of the hybrid filter [Fig. 2(a)] possesses a narrow resonance for tighter locking and the one in the lower branch possesses a broad resonance for obtaining a wide capture range. The resulting hybrid filter thus inherits both properties. The resonance frequencies of the two filter branches must match to ensure the symmetry of the error signal in the vicinity of its zero crossing. The location of the zero crossing determines the exact frequency offset between the lasers, since the feedback loop stabilizes the error signal at the zero value. In our design, a resonance frequency of 22.6 MHz is chosen, such that it is high enough to obtain a sufficiently large capture range but low enough to facilitate easy circuit implementation. Note that although the feedback loop always locks the signal seen by the FD at 22.6 MHz, the actual laser offset frequency is given by the sum of this value and the frequency of the tunable LO.

The frequency of the laser that is to be stabilized is controlled through its injection current. A home-built analog feedback loop utilizing the error signal generated by the FD controls this current with a unity-gain bandwidth of approximately 100 kHz. The loop contains two integrators, with the second one kicking in for frequencies below 20 kHz, giving rise to a $1/\omega^2$ feedback strength down to dc. The implementation of the feedback controller is carried out with particular attention to ground loops, which are typically a major source of stability degradation in many applications. The circuit board is designed such that all inputs and outputs are carried out differentially (interchangeably using AMP03 and LT1167 ICs), cutting ground connections between various devices and hence eliminating ground-voltage shifts across the circuit board. In the implemented frequency feedback, the FD output is directly connected to the feedback controller after 50-Ω termination and some attenuation for loop gain tuning. No low-pass filtering is utilized to eliminate the harmonics of the beat note that the FD additionally generates. Such filtering is observed to shift the locking point—presumably due to back reflections into the FD—but does not seem to noticeably affect the locking stability.

Real-world analog mixers can develop an input-power-dependent residual dc offset in their outputs, even when no mixing to dc is expected in the ideal case [27]. Thus, power fluctuations at the FD—containing a mixer—have the potential to turn into small additive fluctuations in the generated error signal. Since the feedback controller would mistake these for frequency-offset fluctuations, power drifts and fluctuations could lead to degradation of the actual frequency-offset stability. In order to suppress such effects, we first reduce the power fluctuations by saturating the amplifiers leading to the FD (Fig. 1) and, further, utilize additional active feedback stabilization to fix the beat-note power seen by the FD. This feedback circuitry (not shown) splits (Mini-circuits PSC-2-1+) the signal into two paths, self-mixes (SRA-1-1+) the sample branch to

effectively measure the power, and sends the other branch to the FD. A voltage variable attenuator (PAS-3+1) situated before the splitter then stabilizes the power by means of a low-bandwidth feedback loop utilizing the power measurement. Note that the self-mixing is carried out with power levels at least 10 dB below the mixer input saturation point. The printed circuit board housing the FD and the power control circuitry (dashed box in Fig. 1) is operated with a nominal input power of 17 dBm and remains identically functional down to 11 dBm. The amplifier saturation and the active rf power control provide a buffer for potential beat-note power degradations over time (up to 10 dB) without compromising the operational performance.

III. EXPERIMENTAL CHARACTERIZATION

The error signal generated by the FD is characterized by applying a single tone from a function generator while stepping its frequency to map the response [Fig. 2(b)]. The sharp region of the error signal is measured to have a width of 1.8 MHz, in agreement with the design parameters. The lock-capture range is empirically found to be around 190 MHz, ranging from 45 MHz below the unique locking point to 145 MHz above. The error-signal tails extend further than this [Fig. 2(b)] but the noise on the error signal—originating from finite laser line widths—hinders lock acquisition for initial conditions too far from the locking point. In free-running operation, the employed laser systems do not drift by more than approximately 50 MHz, justifying the choice of the design parameters leading to the observed capture range.

The effect of the nonideal behavior of the FD mixer is characterized by measuring the error-signal zero-crossing frequency as a function of the rf input power to the FD unit. Empirically, a "turning point" is identified around 5.2 dBm [Fig. 2(c)], where the zero-crossing frequency is insensitive to the input power. These measurements are carried out with a single tone from a function generator. The exact power corresponding to the "turning point," however, appears to be line width dependent and needs to be fine tuned in locked operation by observing the resulting mean frequency offset between the lasers. With saturated amplifiers and additional active power stabilization at the "turning point," the stability is no longer limited by power fluctuations.

The evaluation of the achieved offset locking stability is carried out by recording the beat-note frequency through the 22.6-MHz monitor output (Fig. 1) using a frequency counter (SRS FS470). Sample time traces with and without power stabilization are shown in Fig. 3(a), displaying the utility of power stabilization. For the power-stabilized case, the mean frequency remains within a 200-Hz window over the course of a day. The characterized frequency-offset instabilities at different time scales for this case are obtained by calculating the Allan deviation [Fig. 3(b)] of

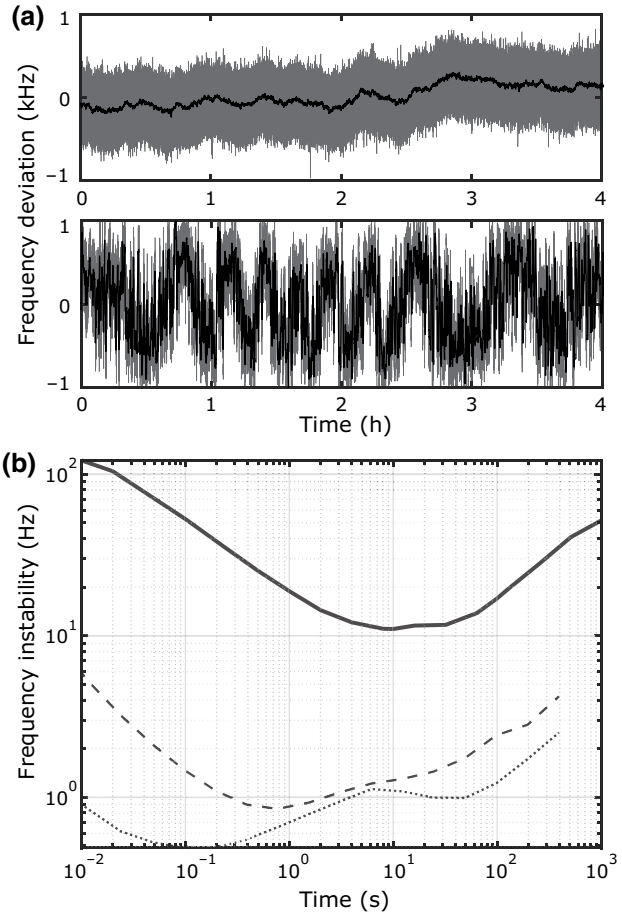

FIG. 3. (a) The deviation of the monitored beat frequency with (upper) and without (lower) power stabilization. Gray, 0.01-s frequency-counter gate time; black, 1-s gate time. (b) The Allan deviation of the observed beat frequency (solid line) for the power-stabilized case. A minimum of 12 Hz at 10 s averaging is reached and the instability remains below 55 Hz for time scales exceeding 1000 s. The dashed line is the instability that would be naively inferred from the recorded residual error signal while the lock is engaged. The dotted line indicates the electronic noise floor inferred by blocking the laser light.

the recorded beat-note data. The instability remains below 55 Hz for more than 1000 s and has a minimum value of 12 Hz at a 10 s time scale. The measured lock tightness inferred from the closed-loop error signal and the limitations induced by detection noise measured in open loop with the lasers blocked [Fig. 3(b)] both contribute at least an order of magnitude lower than the observed frequency-offset instability. The origin of the dominant contribution to the instability is currently unclear.

The agility of user-inducible laser frequency-offset changes is related to the bandwidth of the feedback loop controlling the frequency of the stabilized laser. In the current setup, continuous ramp rates of 200 kHz/μs are achievable robustly. The range of instantaneous frequency jumps, on the other hand, is limited by the capture range of

190 MHz. Such step jumps settle toward the set point with a time constant of order 10 μs, determined by the inverse of the lock bandwidth. The frequency offset can be tuned within a range of 1 GHz, limited by the band-pass filters utilized in the microwave-LO-generation chain. In principle, given a widely tunable LO source, the only limitation to the tuning range is due to the 12-GHz bandwidth of the photodetector (Fig. 1).

IV. DISCUSSION AND CONCLUSIONS

We design and implement a frequency-offset locking method based on hybrid electronic *LC* filters. We stabilize two 780-nm miniature ECDL lasers at a 5.5-GHz offset from each other. With attention to details such as input-power stabilization at the FD and utilization of ground-loop elimination techniques for the feedback controller, we reach a very low difference-frequency-locking instability of 12 Hz at 10 s averaging. Some inherent problems of earlier filter-type implementations are thus circumvented with these additional techniques. The hybrid nature of the FD decouples the problem of the capture range from that of lock tightness. The attained stability, the capture range, and the wide tunability make this scheme very appealing for applications where the relative frequencies need to be stabilized and tuned on demand. In this work, the sharp filter region extending over 1.8 MHz is chosen to make the linear range of the error signal larger than the laser line widths but in principle it can be made substantially narrower. We observe that both the sharpness of the resonance (by trying a different filter) and the reduction of power fluctuations increase the stability.

The specific system in this work is developed to frequency stabilize the cooling and repumper beams for laser cooling and trapping of ^{87}Rb atoms. In the final configuration, one laser (Laser 1 in Fig. 1) would be locked to the $3 \leftrightarrow 4'$ transition of the ^{85}Rb D_2 line via modulation transfer spectroscopy (not discussed). Two additional lasers (only one discussed) would then be locked at 5.5-GHz and 1.2-GHz offsets from Laser 1 using the described methods. These two lasers would drive the $1 \leftrightarrow 2'$ repumping and the $2 \leftrightarrow 3'$ cooling transitions of ^{87}Rb respectively. The agile tunability is intended for the required ramping of the cooling-beam detuning. The achieved stability levels are excessive for the current application; nevertheless, the methods remain general and can be used for other demanding applications.

In this work, there is no differential line-width narrowing for the lasers, since the lock bandwidth is appreciably smaller than the laser line widths. In a system that employs either smaller-line-width lasers or larger-bandwidth feedback, the relative line width can be collapsed to very small values. This will have an immediate impact on the short-term stability, pulling the minimum of the Allan deviation to lower values. Additionally, this could also improve the long-term stability: note that the line center is locked with a 12-Hz instability but the line width is several hundreds of kilohertz. Any changes in the beat line shape could alter the effective line center seen by the FD. Such line-shape changes could originate from the lasers themselves or from the time variation of residual back reflections in the FD, which are known to be frequency dependent. This could cause discrepancies between what is measured by the FD and what is measured by the counter used to verify the stability. A more systematic analysis of the stability limitations can be carried out in the future with a narrow-line beat note. Lastly, although saturation of the amplifiers improves robustness and helps to increase long-term stability, this process inevitably generates higher harmonics. These additional rf tones could potentially result in residual time-varying dc signals at the output of the FD. We do not investigate such mechanisms, which might contribute to the observed instabilities.

A comparison of our work with those of Refs. [26,28] is in order, given that they also utilize *LC*-filter-based frequency discriminators. Note that these references are fundamentally about implementing optical phase locking and, as discussed in Sec. I, OPLLs can achieve subhertz-level frequency instabilities. Being able to directly lock the relative laser phase implies even better stability for the relative frequency. In these references, the *LC* discriminators serve two purposes: to ease the initial phase-lock acquisition and to mitigate the chronic loss of lock occurring due to frequency fluctuations that take the beat note out of the inherently narrow capture range of an analog OPLL that is doing the main locking job. This architecture essentially replaces the more complicated digital phase-frequency detectors utilized in analog-plus-digital low-noise OPLL systems [19]. When operated alone (without the phase-locking part), the *LC* discriminators implemented in Refs. [26,28] only provide reported locking instabilities down to the approximately 2 kHz level, compared to the 12 Hz value reported here. While OPLLs achieving better frequency stabilities can be implemented more easily using lasers with 100-kHz-level line widths, for our near-megahertz-line-width lasers, this requires electronic feedback bandwidths much larger than 1 MHz, posing a significantly bigger challenge. Our presented results constitute a highly stable frequency-locking based on optical beat-note detection without resorting to optical phase locking. It will still be very interesting to incorporate analog phase discrimination to implement additional OPLL functionality in the current system to investigate potential benefits.

ACKNOWLEDGMENTS

This work was supported by Institute of Science and Technology (IST) Austria. We thank Yueheng Shi for technical contributions.

[1] T. Udem, R. Holzwarth, and T. W. Hänsch, Optical frequency metrology, Nature **416**, 233 (2002).

[2] H. J. Metcalf and P. van der Straten, *Laser Cooling and Trapping* (Springer, New York, 1999).

[3] M. Fleischhauer, A. Imamoglu, and J. P. Marangos, Electromagnetically induced transparency: Optics in coherent media, Rev. Mod. Phys. **77**, 633 (2005).

[4] M. Kasevich and S. Chu, Atomic Interferometry Using Stimulated Raman Transitions, Phys. Rev. Lett. **67**, 181 (1991).

[5] J. Hu, A. Urvoy, Z. Vendeiro, V. Crépel, W. Chen, and V. Vuletić, Creation of a Bose-condensed gas of ^{87}Rb by laser cooling, Science **358**, 1078 (2017).

[6] C. Santori, P. Tamarat, P. Neumann, J. Wrachtrup, D. Fattal, R. G. Beausoleil, J. Rabeau, P. Olivero, A. D. Greentree, S. Prawer, F. Jelezko, and P. Hemmer, Coherent Population Trapping of Single Spins in Diamond under Optical Excitation, Phys. Rev. Lett. **97**, 247401 (2006).

[7] J. H. Bodey, R. Stockill, E. V. Denning, D. A. Gangloff, G. Éthier-Majcher, D. M. Jackson, E. Clarke, M. Hugues, C. L. Gall, and M. Atatüre, Optical spin locking of a solid-state qubit, Npj Quantum Inf. **5**, 95 (2019).

[8] A. D. Ludlow, M. M. Boyd, J. Ye, E. Peik, and P. O. Schmidt, Optical atomic clocks, Rev. Mod. Phys. **87**, 637 (2015).

[9] G. M. Tino and M. A. Kasevich, *Atom Interferometry* (IOS Press, Amsterdam, 2014), Vol. 188.

[10] S. S. Szigeti, O. Hosten, and S. A. Haine, Improving cold-atom sensors with quantum entanglement: Prospects and challenges, Appl. Phys. Lett. **118**, 140501 (2021).

[11] F. B. J. Buchkremer, R. Dumke, C. Buggle, G. Birkl, and W. Ertmer, Low-cost setup for generation of 3 GHz frequency difference phase-locked laser light, Rev. Sci. Instrum. **71**, 3306 (2000).

[12] D. M. S. Johnson, J. M. Hogan, S.-w. Chiow, and M. A. Kasevich, Broadband optical serrodyne frequency shifting, Opt. Lett. **35**, 745 (2010).

[13] T. Day, E. Gustafson, and R. Byer, Sub-hertz relative frequency stabilization of two-diode laser-pumped Nd:YAG lasers locked to a Fabry-Perot interferometer, IEEE J. Quantum Electron. **28**, 1106 (1992).

[14] K. Nakayama, M. Hyodo, R. Ohmukai, and M. Watanabe, Multiple frequency stabilization of lasers using double saturation spectroscopy, Opt. Commun. **259**, 242 (2006).

[15] S. C. Bell, D. M. Heywood, J. D. White, J. D. Close, and R. E. Scholten, Laser frequency offset locking using electromagnetically induced transparency, Appl. Phys. Lett. **90**, 171120 (2007).

[16] G. P. Greve, C. Luo, B. Wu, and J. K. Thompson, Entanglement-Enhanced Matter-Wave Interferometry in a High-Finesse Cavity, arXiv:2110.14027 (2021).

[17] D. Nicolodi, B. Argence, W. Zhang, R. Le Targat, G. Santarelli, and Y. Le Coq, Spectral purity transfer between optical wavelengths at the 10^{-18} level, Nat. Photonics **8**, 219 (2014).

[18] G. Santarelli, A. Clairon, S. Lea, and G. Tino, Heterodyne optical phase-locking of extended-cavity semiconductor lasers at 9 GHz, Opt. Commun. **104**, 339 (1994).

[19] L. Cacciapuoti, M. de Angelis, M. Fattori, G. Lamporesi, T. Petelski, M. Prevedelli, J. Stuhler, and G. M. Tino, Analog+digital phase and frequency detector for phase locking of diode lasers, Rev. Sci. Instrum. **76**, 053111 (2005).

[20] U. Schünemann, H. Engler, R. Grimm, M. Weidemüller, and M. Zielonkowski, Simple scheme for tunable frequency offset locking of two lasers, Rev. Sci. Instrum. **70**, 242 (1999).

[21] Y. Hisai, K. Ikeda, H. Sakagami, T. Horikiri, T. Kobayashi, K. Yoshii, and F.-L. Hong, Evaluation of laser frequency offset locking using an electrical delay line, Appl. Opt. **57**, 5628 (2018).

[22] J. Hughes and C. Fertig, A widely tunable laser frequency offset lock with digital counting, Rev. Sci. Instrum. **79**, 103104 (2008).

[23] G. Ritt, G. Cennini, C. Geckeler, and M. Weitz, Laser frequency offset locking using a side of filter technique, Appl. Phys. B **79**, 363 (2004).

[24] G. Puentes, Laser frequency offset locking scheme for high-field imaging of cold atoms, Appl. Phys. B **107**, 11 (2012).

[25] N. Strauß, I. Ernsting, S. Schiller, A. Wicht, P. Huke, and R.-H. Rinkleff, A simple scheme for precise relative frequency stabilization of lasers, Appl. Phys. B **88**, 21 (2007).

[26] W.-Y. Cheng, T.-J. Chen, C.-W. Lin, B.-W. Chen, Y.-P. Yang, and H. Y. Hsu, Robust sub-millihertz-level offset locking for transferring optical frequency accuracy and for atomic two-photon spectroscopy, Opt. Express **25**, 2752 (2017).

[27] E. Rubiola, Tutorial on the double balanced mixer, arXiv:0608211 [physics] (2006).

[28] Y. Seishu and T. Hasegawa, Robust offset locking of laser frequency with electronically tunable *LC* circuits for sub-millihertz uncertainty, Appl. Phys. B **125**, 142 (2019).